RSC Advances

ROYAL SOCIETY OF CHEMISTRY

www.rsc.org/advances

Cite this: DOI: 10.1039/c0xx00000x

www.rsc.org/xxxxxx

ARTICLE TYPE

Solution Based Rapid Synthesis of $AgCuO_2$ at Room Temperature

Padmavathy, N.†; Vijayaraghavan, R*†; Giridhar U. Kulkarni‡

Received (in XXX, XXX) Xth XXXXXXXXX 20XX, Accepted Xth XXXXXXXXX 20XX
DOI: 10.1039/b000000x

We report a single step synthesis of $AgCuO_2$ within minutes resulting in a poly crystalline, single phasic product crystallizing in monoclinic system. Chemical composition analysis has confirmed the stoichiometry of the product with oxygen in slight excess (~ 0.1). Growth of this oxide, involved cuboidal nanoparticles in the initial stages and needle-like microstructures in the end, as shown by scanning electron microscopy. The novelty of the method lies in the stabilization of Cu in the 3+ state under ambient conditions in a rapid aqueous process.

1. Introduction

Oxide materials crystallizing in a variety of structures and exhibiting many useful physical and chemical properties have been investigated more intensively since the break-through discovery of high temperature superconductivity in perovskite related cuprates in 1986.[1,2] The salient structural features of these oxides are attributed to the abilities of the metal ions to exhibit different coordination numbers and the resultant polyhedral networks. Among the transition metal ions, copper exhibits 1+ and 2+ oxidation states, in general, and 3+ rarely, and can form square planar, square pyramidal and octahedral coordination polyhedra in cuprates.[3] Cu formally exists in 3+state only in few compounds like $ACuO_2$ (A=Na, K) and $LaCuO_3$ and in superconducting cuprates, as mixed valent Cu^{2+} /Cu^{3+} or as $[Cu\text{-}O]^{+}$ [4-6]. The highest Tc of 164 K is held by Hg-Cu oxides under high pressure.[7] Ag with its similarity to Hg in its chemistry and coordination can be a possible substitute for Hg in Hg cuprates. This led to the discovery of two ternary silver copper oxides, namely, $Ag_2Cu_2O_3$ with 3D structure having Ag and Cu in 1+ and 2+ oxidation states respectively and $AgCuO_2$ with layered 2D structure, notably, with Cu in 3+ state[8,9]

Among these, $AgCuO_2$ is an interesting layered oxide with silver in dumb- bell shaped linear (two) coordination and Cu in square planar (four) coordination. The excess charge on Ag (1+δ) and copper (2+δ) is delocalized and spread on to oxygen as well[10,11]. Due to mixed valency it is expected to exhibit semiconducting/metallic property and is therefore being explored for a variety of applications such as photovoltaics and batteries[12, 13]. The synthetic procedures adopted for $AgCuO_2$ are i) wet chemical oxidation at 90 ºC ii) electrochemical oxidation of $Ag_2Cu_2O_3$ with intercalation of oxygen iii) ozone oxidation of aqueous suspensions of $Ag_2Cu_2O_3$ for extended periods and iv) hydrothermal method using AgO as an oxidizing agent with $CuSO_4$ for 17h [14-16]. These methods involve either longer reaction time, elevated temperature or harsh conditions and it calls for an alternative soft chemical method, involving milder conditions as well as short reaction time. We considered it worthwhile to explore in this direction, particularly in respect of $AgCuO_2$ in which Cu formally exists in its highest oxidation state. The report by McMillan in 1962 that alkaline solution of Ag^{1+} ions in the presence of persulfate yields the corresponding higher valent silver oxides prompted us to adopt a similar procedure under ambient conditions to prepare the ternary oxide, $AgCuO_2$ from the corresponding Ag and Cu solutions.[17] Indeed, we are successful in obtaining single phasic and well- crystalline $AgCuO_2$, within 5 minutes in a single step one-pot synthesis at room temperature (RT). More importantly, $AgCuO_2$ obtained by this method is found to contain excess oxygen of 0.10 per formula unit, in which Cu is expected to be fully oxidized as Cu 3+ or as [Cu-O]+. To the best of our knowledge, this is the first report on room temperature synthesis of a layered cuprate with Cu partly in 3+ state.

2. Experimental Section

2.1. Raw Materials.

Silver acetate (Aldrich) and copper acetate (Fluka), Potassium persulfate, and NaOH (Sd-Fine) were purchased and used as received with a purity of 99.9%. $AgCuO_2$ was harvested by drop casting the suspension drawn from precursor solution at regular intervals of time, on glass slide followed by drying at room temperature.

2.2. Characterization.

Powder X-ray diffraction (XRD) was used to identify the phase, its purity and to determine the crystallite size. XRD was recorded using Bruker D8 –Advanced diffractometer with Cu Kα (λ= 1.5406 Å) radiation.

The particle size and morphology were studied by Field Emission Scanning Electron Microscopy (FESEM) and Transmission Electron Microscopy (TEM).The images were recorded with a FEI Nova Nano SEM 600 and low vacuum imaging was performed on the same instrument using helix detectors. Energy-dispersive spectroscopy (EDS) analysis was performed with an EDAX Genesis instrument (Mahwah, NJ) attached to the SEM

column.

Transmission Electron Microscopy (TEM) was carried out with a JEOL-3010 instrument operating at 300 kV (λ = 0.0196 Å) and electron diffraction (ED) patterns were collected at a camera length of 20 cm (calibrated with respect to the standard polycrystalline Au thin film). $AgCuO_2$ samples for TEM and ED were prepared by dispersing the sample in acetone and drop-casting the solution on a carbon-coated grid.

X-ray Photoelectron Spectra (XPS) of the samples were recorded with an ESCALAB MKIV spectrometer employing AlKα radiation (1486.6 eV).

Optical measurements were carried out at room temperature with a Perkin Elmer model Lambda 900 UV/Vis/NIR spectrometer. The transmittance of $AgCuO_2$ was measured in specular and diffusive modes with integrated sphere.

Thermo Gravimetric Analysis (TGA) was carried out with a Mettler Toledo Star instrument (Weinheim, Germany) in the temperature range 30 – 500 °C in N_2 atmosphere with a heating rate of 10 °C/min. Oxygen content was estimated by Iodometric titrations.

2.3. Synthesis of $AgCuO_2$

Here we describe the novel synthetic route of $AgCuO_2$. Aqueous solutions of equal volumes of equimolar copper acetate and silver acetate were separately prepared and then mixed. Separately, aqueous NaOH was prepared with twice the concentration containing small amount of $K_2S_2O_8$ as an oxidizer. This alkaline persulfate solution was then slowly added to the metal acetate solution with stirring. The whole solution turned black immediately indicating the formation of the product in suspension. At one minute intervals, aliquot (2mL) were drawn from the parent solution into a beaker and was then washed thoroughly with distilled water until the pH reached neutral value. The precipitated products thus harvested at each time interval from the parent solution were characterized by XRD and FESEM. The schematic representation of the typical procedure is depicted in (Figure 1a). The yield of the product was 89%.

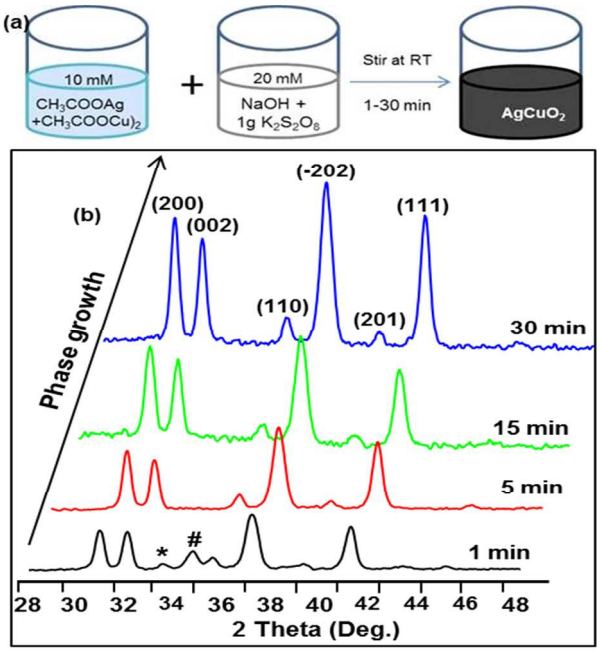

3. Results and Discussion

The XRD patterns (Fig. 1b) reveal the formation of single phasic $AgCuO_2$. Interestingly, the sample extracted from the parent alkaline persulfate solution just after one minute of the reaction, already contained a significant amount of the product, $AgCuO_2$ with minor impurities. By the end of 5 minutes, the reaction was complete giving rise to a single phasic $AgCuO_2$. The intensities of the characteristic reflections (200), (002), (202) and (011) (Fig. 1b) of $AgCuO_2$ increased with reaction time indicating the growth of $AgCuO_2$ with increasing crystallinity. A typical XRD pattern of the product harvested from the fifth minute (Fig. 2) can be indexed to a monoclinic system with the refined lattice parameters of a = 6.014 (3) Å; b = 2.818 (5) Å; c = 5.892 (4) Å; β= 107.98° The JCPDS values are a = 6.076 Å; b = 2.809 Å; c = 5.873 Å; β = 107.99° corresponding to stoichiometric bulk $AgCuO_2$.

Fig. 1. (a) Schematic representation of RT synthesis of $AgCuO_2$. (b) XRD patterns of products formed at various time intervals. The single phasic $AgCuO_2$ formed after 5 minutes could be indexed with JCPDS 01-070-8903.The product formed after one minutes contained minor impurities, Ag_3O_4(*) and $Cu(OH)_2$ (#).

Clearly, we note a decrease in "a" parameter and an increase in "c" parameter in oxygen excess $AgCuO_{2.1}$ comparing with JCPDS data indicating oxidation of copper well over 2+ in the ab plane and intercalation of oxygen in between the layers increasing the "c" parameter. This is consistent with the observation in cuprates like La_2CuO_4[18].

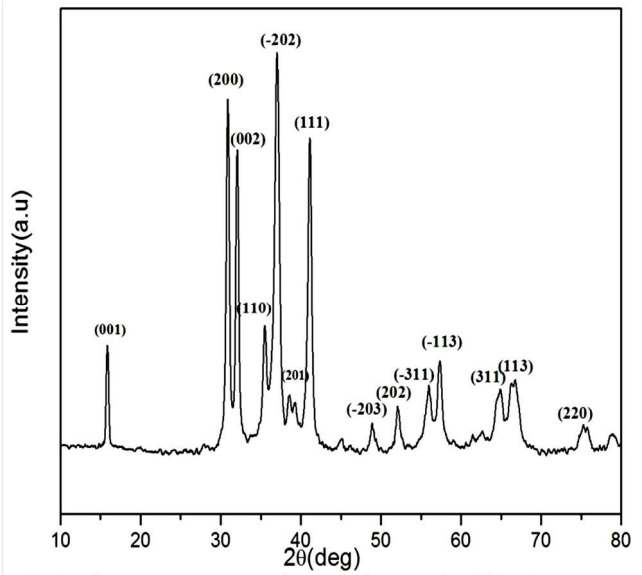

Fig. 2. Full range XRD pattern of AgCuO2 harvested at fifth minute.

It is indeed amazing that this simple precipitation method leads to unusual Cu 3+ along with the usual Cu 2+, which may be due to in-situ oxidation of the latter caused by the prevalent persulfate. The fact that it all completes within minutes at room temperature indicates that the reaction must be kinetically controlled. Our method therefore differs significantly from the earlier reports[14-16].

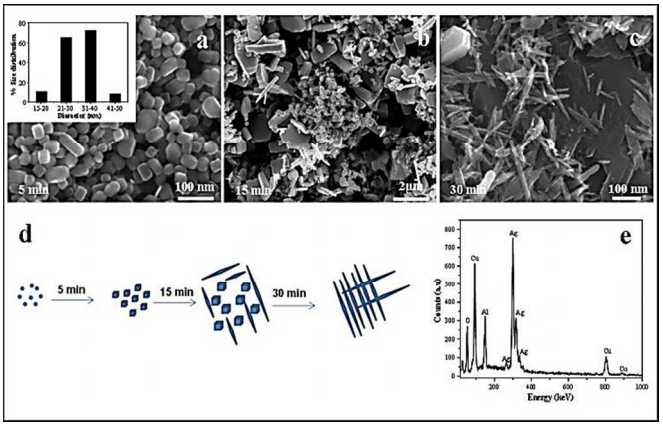

Fig. 3. (a) FESEM images of $AgCuO_2$ at (a) 5 min (b) 15 min (c) 30 min of synthesis showing progressive growth of cuboidal particles into needle-like structures. Inset in (a) shows the histogram of particle size distribution. (d) Scheme showing growth of cuboidal particles into needle-like structures. (e) EDS spectrum of $AgCuO_2$.

FESEM images (Fig. 3) reveal the growth of $AgCuO_2$ particles with reaction incubation. The product obtained at fifth minute mainly consisted of cuboidal nanoparticles (mean size ~ 30 nm, see Fig. 3a) and after 15 minutes, anisotropic particles - truncated larger plates, rods, and polyhedral plates, were obtained (Fig. 3b). In Fig. 3c, nanorods with larger aspect ratios, an edge length of 200–350 nm and a diameter of 20-40 nm, can be observed from the 30 min product. Fig. 3d depicts a scheme of the growth of nanoparticles into needle-like morphology characteristic of monoclinic system.

Further characterization was carried out on the fifth minute product. The large area EDS spectrum of $AgCuO_2$ (Fig. 3e) confirmed the ratio of Ag to Cu as 1:1. The oxygen content estimated by iodometric titration was found to be 2.15±0.05 per formula unit.

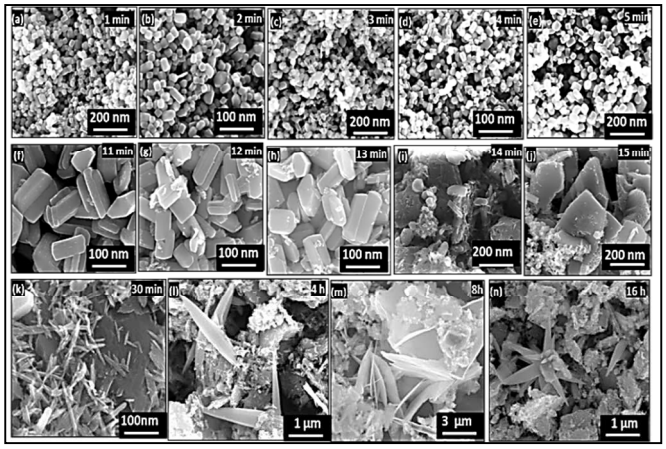

Fig. 4. FESEM images of $AgCuO_2$ (a-e) harvested from mother liquor from 1st -5th min. (f-j). 11th -15th min. (k-n) 30th min - 16h.

FESEM images (Fig. 4) revealed the growth of the product up to 16 h differing in their particle morphology . While products harvested at 1st - 5th minute consisted mostly of spherical nanoparticles (mean size of 30 nm) (Fig. 4a -e), larger particles of 100 – 250 nm (Fig. 4f-j) are observed between 11th – 15th minute. During 30thmin – 16 h (Fig. 4 k-n) anisotropic particles (truncated larger plates, rods, and polyhedral plates) were identified. In Fig. 4k, rod-shaped nanoparticles with larger aspect ratios, with an approximate mean edge length of 200–350 nm and a mean diameter of 20-50 nm, can be seen.

The growth of different morphological structures of $AgCuO_2$ could depend on the reactant to oxidant ratio, reaction time, and temperature. In the present work, with the ratio of silver to copper acetates equal to 1:1 with 1.3 g of persulfate, the growth of our $AgCuO_2$ product with time is controlled by the dehydration of the possible hydroxide precursor $AgCu(OH)_4$ at room temperature through the different crystallographic facets resulting in different nanostructures[19]. Attempts are being made to isolate the hydroxide precursor. More importantly, cuboidal structures of $AgCuO_2$ (Fig. 4a-e) are obtained without the use of the templates. It is to be noted that a variety of nano and microstructures of Cu_2O and Ag_2O have been synthesized by wet chemical methods[20].

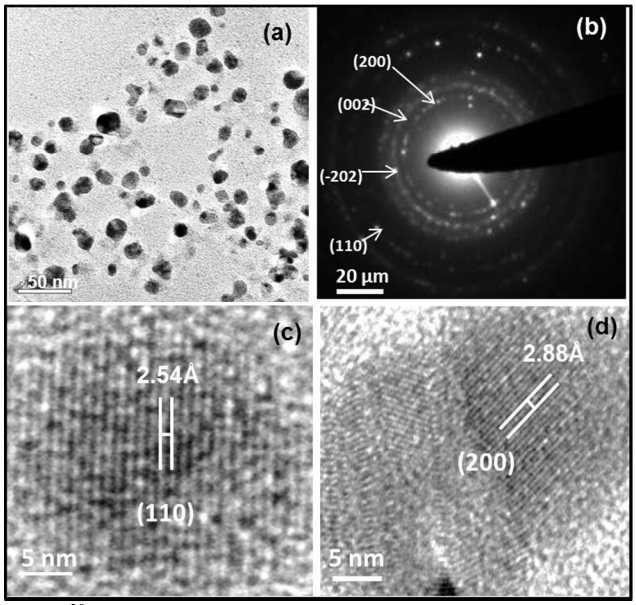

Fig. 5.(a) TEM image of $AgCuO_2$ nanoparticles. (b) Indexed SAED pattern of $AgCuO_2$ reveals polycrystalline nature of the sample. (c) and (d) HRTEM images of the different planes of $AgCuO_2$.

Fig. 5a and 5b show representative TEM micrograph of the $AgCuO_2$ nanoparticles and the corresponding Selected Area Electron Diffraction (SAED) pattern, respectively. Among the particles examined (Fig.5a), more than 70% belonged to the size range of 30 - 40 nm. SAED pattern. (Fig. 5b) of these particles contains diffusive rings, which may be attributed to small polycrystalline grains of the product.

The diffraction features are consistent with the crystalline structure of bulk $AgCuO_2$, corresponding to the diffraction planes of (200) and (110). High-resolution TEM images (Fig. 5c and d) show lattice planes corresponding to $AgCuO_2$.

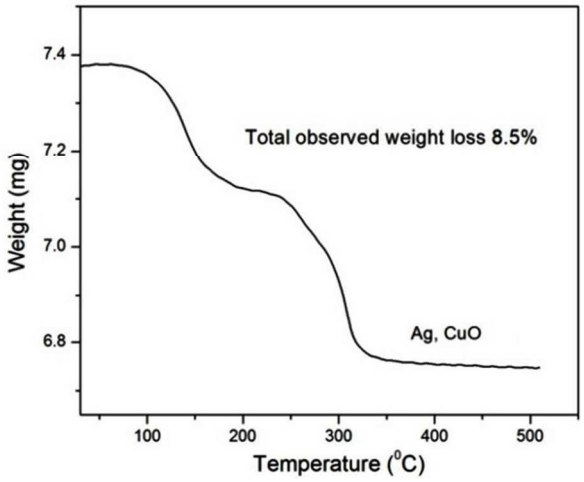

Fig.6. Thermogram of $AgCuO_2$ under N_2 atmosphere.

Thermogravimetric data shown in Fig. 6, exhibits three distinct weight losses up to 350˚C, the final products being Ag and CuO (confirmed by XRD, see supporting information Fig. S1). The observed total weight loss (up to stable final product formation) of 8.5%, is close to the theoretical weight loss of 8.58% indicating that the starting composition to be $AgCuO_{2.10\pm0.02}$ in agreement with chemical titration (2.10±0.05).

Our soft chemical synthetic method under ambient conditions has resulted in an oxygen excess of 0.10 per formula unit ($AgCuO_{2.10}$) which gets intercalated in between the layers of $AgCuO_2$, whereas in other cuprates such as La_2CuO_4 and Sr_2CuO_3, oxygen intercalation takes place only under high pressure or in electrochemical conditions.[18,21]

X-ray Photoelectron Spectra (XPS) of $AgCuO_{2.10}$ were recorded to obtain the binding energies of Ag, Cu and oxygen. The survey spectrum is shown Fig. 7a. Fig. 7b shows the Ag 3d core level spectrum exhibiting the Ag $3d_{5/2}$ and Ag $3d_{3/2}$ peaks at the binding energies of 367.1 e V and 373.3 eV respectively. It may be noted that the binding energies of $3d_{5/2}$ lies between 367.5 – 367.7 eV in the reference compound of Ag_2O (Ag in 1+) and around 367.1 – 367.4 eV with a satellite at 366.2 eV in the reference compound AgO corresponding to Ag in 1+ and 3+ states respectively[22-24]. Fig. 7b indicates that Ag in $AgCuO_{2.10}$ is oxidized more than 1+, possibly with a delocalization of the excess charge. The width (FWHM) of Ag $3d_{5/2}$ in $AgCuO_2$ is found to be 1.09 eV, less than that found in Ag(I) oxide (FWHM 1.2 eV)[23] indicating that Ag in $AgCuO_{2.10}$ is oxidized more than 1+. Cu 2p 3/2 spectrum (Fig.7c) shows a peak around 934.7 eV and a shoulder at 933.8 eV indicating the presence of Cu 2+ and 3+ respectively. These values correspond closely to Cu 2p 3/2 binding energies in CuO[25] and $NaCuO_2$[26].

The least square fit (Gaussian) for the O1s peak of $AgCuO_2$ (Fig. 7d) gives three components with binding energies of 528.6, 530.6 and 532.8 eV.

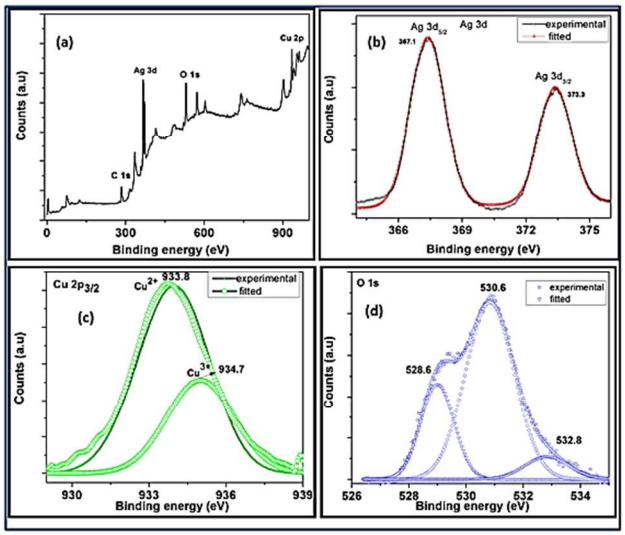

Fig. 7. XPS survey spectrum (a) and core level spectra of (b) Ag3d, (c) Cu2p (d) O1s of $AgCuO_{2.10}$.

These values are in close agreement with earlier report[10]. It is to be noted, the binding energies of O^{2-}, O_2^{2-} and O_2^{-} species in oxides occur at 530.5, 532.5 – 533.5 and 534.5 – 535.5 eV respectively[27]. It indicates that in our $AgCuO_{2.10}$, the excess charge on Cu (more than 2+) and Ag (more than 1+) is delocalized onto oxygen also as we observed a peak at 532.8 eV corresponding to peroxide species.

Assuming a formula of $AgCuO_2$ one would expect Ag to be in 1+δ and Cu to be in 2+ δ (δ varying between 0 to 1). The excess charge could be delocalized on to oxygen also; however, in our $AgCuO_{2.10}$ the excess oxygen could oxidize Ag or Cu more than that found in bulk $AgCuO_2$[10]. Since we find the evidence for the presence of peroxide, the formula along with the charges could be represented as $(Ag^{1+x}Cu^{2+y}\{O^{2-}, O_2^{2-}\}^{-(4.2+2\delta)})_{2.10}$.

Optical band gap estimated from optical absorption of $AgCuO_2$ (Fig. S2) using Tauc's relation from the plot of $(\alpha h\upsilon)^2$ vs photon energy ($h\upsilon$) was found to be 1.84 eV. Our $AgCuO_{2.10}$ product shows a conductivity value of 100 - 500 mhos. cm^{-1} at room temperature consistent with an earlier report[28]. However, this value of conductivity is lower than that of high temperature superconducting cuprates. Due to poor grain connectivity, the resistivity is higher than expected from complete delocalization. We are looking into the correlation of the electronic structure of $AgCuO_{2.10}$ to its properties.

4. Conclusions

Our synthetic approach based on aqueous persulfate oxidation at room temperature has successfully resulted in pure, stable, nanocrystalline $AgCuO_2$ in a few minutes. In the initial stages, the nanoparticles are found to be cuboidal in shape which grow into needle-like crystals of few μm size. The present study has significance as $AgCuO_2$ is an interesting material with low band gap and more importantly, with Cu in the unusual 3+ state. This method has also resulted in soft intercalation of oxygen (up to 0.10 per formula unit) into $AgCuO_2$ under ambient conditions, which otherwise may require high pressure. The method also results in different morphological structures of $AgCuO_2$. The present method also opens up possibilities for rapid, soft-

chemical synthesis of many other multinary oxides.

Notes and references

Supporting Information

Optical band gap determination of $AgCuO_2$ and XRD of intermediate and final products of thermal analysis of the title oxide are given.

AUTHOR INFORMATION

† Materials Chemistry Division, School of Advanced Sciences, VIT University, Vellore, Tamil Nadu 632 014, India

‡ Chemistry & Physics of Materials Unit and Thematic Unit on Nanochemistry, Jawaharlal Nehru Centre for Advanced Scientific Research, Jakkur, Bangalore 560 064, India.

Corresponding Author

rvijayaraghavan@vit.ac.in

ACKNOWLEDGMENT

The authors thank Prof. C.N.R. Rao and Prof. M. Jansen for useful discussions and encouragement. PN and VR thank VIT University for support. GUK thanks DST for funding.

1. C. N. R. Rao and B. Raveau, Transition Metal Oxides: Structure Properties and Synthesis of Ceramic Oxides, 2nd edition NY 1998, Wiley-VCH, Weinheim.
2. J.G. Bednorz, and K.A. Z. Muller, *Phys. B. Condens. Matter*, 1986, **64**, 189-193.
3. J. Paul Attfield, *J. Mater. Chem*. 2011, **21,** 4756-4764.
4. T. L. Fredman, and A.M. Stacy, *J. Solid State Chem,* 1984, **109**, 203-204.
5. G. Demazeau, C. Parent, M. Pouchard and P. Hagenmuller, *Mat. Res. Bull,* 1972, **7,** 913 – 920.
6. W. K. Ham, G. F. Holland, A. M. Stacy, *J. Am. Chem. Soc,* 1988, **110,** 5214 -5215.
7. L. Gao, Y. Y. Xue, F. Chen, Q. Ziong, R. L. Mentg, D. Ramirez, C.W. Chu, J.H. Eggert and H.K. Mao, *Phys. Rev B,* 1994, **50,** 4260-4263.
8. P. Gomez –Romero, E.M. Tajeda-Rosales and M. Rosa Palacin, *Angew. Chem,* 1999, **111**, 544-546.
9. J. Curda, W. Klein, H. Liu and M. Jansen*, J. Alloys Compds*, 2002, **338,** 99-107.
10. D. Munaz-Rojas, G. Subias, J. Frexedas, Pedro-Gomez Romero and N. Casan-Pastor, *J. Phys. Chem,* 2005, **109,** 6193-6199.
11. D. Munaz-Rojas, J. Frexedes, J. Oro, Pedro-Gomez Romero and N. Casan Pastor, *Cryst. Engg.,* 2002, **5,** 459-463.
12. P. Sauvage, D. Munaz-Rojas, K.R. Poeppelmeier and N. Casan-pastor, *J. Solid State Chem*, 2009, **182,** 174-175.
13. J. Feng, B. Xiao, C.T. Zhou, Y.P. Du and R. Zhou, *Solid State Comm,* 2009, **149,** 1569-1573.
14. J. Curda, W. Klein and M. Jansen, *J. Solid State Chem,* 2001, **162,** 220 - 224.
15. D. Munaz-Rojas, G. Subias, J. Frexedas, Pedro-Gomez Romero and N. Casan-Pastor, *J. Solid, State Chem,* 2005, **178,** 295-305.
16. D. Munaz-Rojas, R. Cordoba, Amalio Ferdandey – Pecheco, J. M. D. Terefa, G. Sauthier, J. Frexdes, R.I. Walton, R. Pastor, N. C. *Inorg. Chem,* 2000, **49,** 10977 – 10979.
17. J.A. McMillan, *Chem. Rev*, 1962, **62**, 65 – 80.
18. J.E. Schirber, W.R. Bayless, F.C. Chou, D.C. Jhonston, P.C. Canfield and Z. Fisk, *Phys. Rev. B* 1993, **48,** 6506- 6508.
19. W.P. Liao and J.J. Wu, *J. Mater. Chem.,* 2011, **21**, 9255-9262.
20. J. Ren, W. Wang, S. Sun, L. Zhang, L. Wang, and J. Chang , *Ind. Eng. Chem. Res.*, 2011, **50**, 10366–10369.
21. Q.Q. Liu, H. Yang, X.M. Qin, Y. Yu, L.X. Yang, F.Y. Li, R.C. Yu, C.Q. Jin and S. Uchida, *Phys. Rev B,* 2006**, 74**, 100506 (R).
22. L. H. Tjeng, M. B. J. Meinders, J. Vanelp, J. Ghijsen, G. A.Sawatzky and R. L. Johnson, *Phys. Rev. B,* 1990, **41**, 3190- 3199.
23. T.C.Kaspar, T. Droubay, S. A. Chambers and P.S. Bagus, *J. Phys. Chem. C*, 2010, **114,** 21562–21571.
24. J. F. Weaver and G. B. Hoflund, *J. Phys. Chem.* 1994, **98,** 8519 - 8524.
25. J. Ghijsen, L.H. Tjeng, J. van Elp, H. Eskes, J. Westerink, G.A. Sawatzky, M.T. Czyzyk, *Phys. Rev. B,* 1988, **38,** 11322 – 11330.
26. P. Steiner, V. Kinsinger, I. Sander, B. Siegwart, S. H¨ufner, C. Politis, R. Hoppe, and H. P. Muller. *Z. Phys. B*, 1987, **67**, 497–502.
27. S.L. Qiu, C.L. Lin, J.Chen and M. Strongin, *J. Vac. Sci. Tech. A,* 1990**, 8,** 2596-2598.
28. J.F.Pierson,D.Wiederkehr, J.M. Cahppe and N.Martin. *Appl. Surf. Scinece*, 2006, **253**, 1484 – 1488.